ELSEVIER

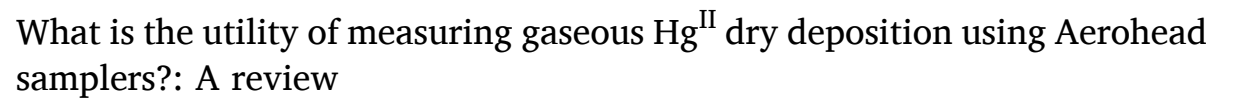
Contents lists available at ScienceDirect

# Science of the Total Environment

journal homepage: www.elsevier.com/locate/scitotenv



# Review





Mae Sexauer Gustin <sup>a,\*</sup>, Sarrah M. Dunham-Cheatham <sup>b</sup>, Stefan Osterwalder <sup>c,d</sup>, Olivier Magand <sup>e</sup>, Aurélien Dommergue <sup>c</sup>

- a Department of Natural Resources and Environmental Science, University of Nevada, Reno
- <sup>b</sup> College of Biotechnology, Natural Resources and Environmental Science, University of Nevada, Reno
- CUniv. Grenoble Alpes, CNRS, INRAE, IRD, Grenoble INP (Institute of Engineering and Management Univ. Grenoble Alpes), IGE, 38000 Grenoble, France
- <sup>d</sup> Department of Environmental Systems Science (D-USYS), Institute of Agricultural Sciences, ETH Zurich, Zurich, Switzerland
- e Observatoire des Sciences de l'Univers à La Réunion (OSU-R), UAR 3365, CNRS, Université de La Réunion, Météo France, 97744 Saint-Denis, La Réunion, France

#### HIGHLIGHTS

- To understand Hg inputs to ecosystems dry and wet deposition must be measured.
- Aerohead samplers are a viable method for measurement of dry deposition.
- Large-scale trends in dry deposition can be determined using this method.
- This method also provides a means of determining deposition sources.
- Use of Aerohead samplers allows for assessment of success of Minamata Convention.

#### GRAPHICAL ABSTRACT



### ARTICLE INFO

Editor: Jay Gan

Keywords: Cation exchange membranes Gaseous oxidized mercury Deposition velocities Regional trends

### ABSTRACT

The most efficient way to quantify  $Hg^{II}$  inputs to ecosystems is to measure wet and dry deposition. Wet deposition of  $Hg^{II}$  is determined by measuring Hg concentrations and the volume of precipitation. Dry deposition of  $Hg^{II}$  is determined through direct measurement and/or determined indirectly by measuring air concentrations and using model-generated deposition velocities. Here, data collected using an Aerohead sampler holding cation exchange membranes are summarized, and the utility of this method for understanding dry deposition, and other measurements and processes is discussed. This analysis includes information from publications, and recent data collected at Guadalupe Mountains National Park, Texas, USA, and Amsterdam Island, Southern Indian Ocean. This method primarily measures gaseous  $Hg^{II}$  and little particulate-bound Hg. The Aerohead method is useful for looking at large-scale trends in deposition, verifying Hg depletion events, calculating dry deposition velocities for compounds with specific chemistry, and identification of sources of  $Hg^{II}$ . At numerous locations in the western USA, deposition rates were greater at higher elevations due to elevated concentrations associated with long-range transport of atmospheric pollution. When used in tandem with the Reactive Mercury Active System or a

E-mail address: mgustin@unr.edu (M.S. Gustin).

<sup>\*</sup> Corresponding author.

#### 1. Introduction

Mercury (Hg) exists in the atmosphere as gaseous elemental Hg (GEM), gaseous oxidized Hg (GOM, Hg<sup>II</sup>), and particulate-bound Hg (PBM). Hg is distributed globally by atmospheric transport and deposited to ecosystems by way of wet and dry processes. The contribution of wet versus dry deposition varies depending on location. For example, wet deposition greatly exceeded dry deposition in Florida; however, in Nevada, dry deposition was much higher (Sather et al., 2013). Wet deposition is measured by multiple networks (e.g., European Monitoring and Evaluation Programme, Global Mercury Observation System; National Institute for Minamata Disease; National Institute for Environmental Studies (Japan); and National Atmospheric Deposition Program (USA)), and typically entails measurement of the concentration of Hg in the precipitation and the volume of precipitation weekly, biweekly, and in some cases irregular intervals (Prestbo and Gay, 2009; Sprovieri et al., 2017).

For the past 20 years, the Tekran 2537/1130/1135 speciation system (Tekran) has been used to measure GEM, GOM, and PBM (<2.5  $\mu m$ ), respectively. It now has been clearly demonstrated that  $Hg^{II}$  measurements are biased low (Dunham-Cheatham et al., 2023), the PBM measurement suffers from artifacts (c.f. Talbot et al., 2011), and the particulate filter collects  $Hg^{II}$  (Gustin et al., 2013; Allen et al., 2023). More recently, work with using a  $Hg^{II}$  calibrator has demonstrated that when  $HgBr_2$  is permeated onto the quartz fiber filter used to collect PBM in the Tekran,  $Hg^{II}$  is reduced to GEM (Allen et al., 2023). Because Tekran  $Hg^{II}$  data have demonstrated inaccuracies, the accuracy of dry deposition calculations made by models using this data is now of concern.

Dry deposition of Hg<sup>II</sup> can be measured using surrogate surfaces. Methods that have been applied include use of artificial turf (Hall et al., 2017), knife edge and Frisbee samplers (Huang et al., 2011), dry deposition plates (Fang et al., 2013), a circulating water bath that faced up (Sakata and Marumoto, 2005), and a flat plate collector that faced up (Caldwell et al., 2006). For a summary of these methods, see the review by Huang et al. (2014). The above cited review concluded, at that time, that a good dry deposition sampler should reflect the turbulence and deposition velocity of a compound, and that the Aerohead sampler developed by Lyman et al. (2009) with down-facing exposure, was the best available dry deposition plate for HgII deposition. They also reported deposition rates measured using a cation exchange membrane (CEM) in the Aerohead were higher than that determined using Tekran Hg<sup>II</sup> concentrations and a dry deposition model. In Huang et al. (2014), and others, this lack of agreement was thought to be due to the low surface resistance of the membrane. We now know that the CEM deposition measurements are more reliable, due to issues with the Tekran system (Dunham-Cheatham et al., 2023). Dry deposition velocities used in models can also have large uncertainties (Zhang et al., 2023). Dry deposition is calculated using the following equation:

Dry deposition (ng m<sup>-2</sup> h<sup>-1</sup>) = mass on surface (ng)  

$$\div$$
 (surface area (m<sup>2</sup>) × time (h)). (1)

Another parameter to consider that is important for understanding inputs to ecosystems is deposition velocities, that are developed using models. These velocities are then used with surface concentrations to quantify dry deposition. Since Tekran  $Hg^{II}$  concentrations are biased low, accurate measurements of  $Hg^{II}$  concentrations are needed to more accurately calculate  $Hg^{II}$  deposition. Two alternate methods have been developed for measurement of  $Hg^{II}$  concentrations, including dual-channel systems and the Reactive Mercury Active System (RMAS) that

uses membranes (Luippold et al., 2020). Dual-channel systems use one Tekran 2537 module and has two channels, one that measures GEM and the other total gaseous Hg (TGM), allowing for calculation of Hg<sup>II</sup> concentrations by difference (Dunham-Cheatham et al., 2023). Using a dual-channel system or RMAS would allow for calculation of more accurate deposition velocities, that will be lower than previously calculated and reported. Given that the RMAS also allows for identification of compounds, deposition velocities can be estimated for specific compounds. Deposition velocities are calculated using the following equation:

Deposition velocity 
$$(m h^{-1}) = dry deposition (ng m^{-2} h^{-1})$$
  
 $\div air concentration (ng m^{-3}).$  (2)

In this case, dry deposition would be measured by the Aerohead sampler over one to two weeks. The RMAS would concurrently measure Hg concentrations. The limitation here is that the CEM in the RMAS measures GOM and PBM.

Zhang et al. (2009) noted that  $\mathrm{Hg^{II}}$  deposition observations are limited and have large uncertainties, and provided a range of deposition velocities from 0.5 to 6 cm s<sup>-1</sup>. Compilation of the very limited data for PBM indicated values in the range of 0.02 to 2 cm s<sup>-1</sup>. GEM deposition velocities ranged from 0.1 to 0.4 cm s<sup>-1</sup> over vegetated surfaces and wetlands, and were lower over non-vegetated surfaces and soils below canopies. It is noteworthy that their calculated deposition velocities were based on surrogate surface data, and micrometeorological data and concentrations were determined using a Tekran system. Thus, deposition velocities are biased high.

Zhang et al. (2019) provided a range of modeled deposition  $\mathrm{Hg^{II}}$  velocities ranging from 0.65 to 1.89 cm s<sup>-1</sup>, depending on the land use category. In addition to reflecting atmospheric turbulence, Zhang et al. (2019) noted a correlation of dry deposition of  $\mathrm{Hg^{II}}$  with elevation. Huang and Gustin (2015), Wright et al. (2014), and Gustin et al. (2023) reported higher  $\mathrm{Hg^{II}}$  concentrations at higher elevations in the western ISA.

Here, new and published dry deposition data collected using the Aerohead sampler with CEM are compiled and presented. Because the Aerohead membrane consists of the same material in each study, a direct comparison across field sites is possible. What has been learned regarding this sampling method and its utility over the past 16 years is discussed. In addition, we test the hypotheses that variation in the Aerohead dry deposition measurements reflects the chemistry of the compounds present, and that calculated deposition velocities using concentrations measured using the RMAS and deposition determined with the Aerohead samplers reflect the chemistry of the compounds.

# 2. Methods

# 2.1. Field sites - published data

Researchers have deployed and reported measured and/or calculated deposition rate results from Aerohead samplers over the past 16 years (Fig. 1; Table S1). The field sites from these studies were located in, from west to east across the USA: Point Reyes National Seashore, California (CA) (Wright et al., 2014); Elkhorn Slough, CA (Wright et al., 2014); Lick, CA (Wright et al., 2014); Chalk Mountain, CA (Wright et al., 2014); Chews, CA (Wright et al., 2014); Hetch Hetchy Reservoir, CA (Wright et al., 2014); Yosemite National Park, CA (Wright et al., 2014); Sequoia National Park, CA (Wright et al., 2014); Reno, Nevada (NV) (Lyman et al., 2009); Paradise Valley, NV (Lyman et al., 2009); Great Basin National Park, NV (Wright et al., 2014); Pensacola, Florida (FL)

(Lyman et al., 2009; Peterson et al., 2012; Gustin et al., 2012); Yorkville, Georgia (GA) (Lyman et al., 2009); Tampa, FL (Peterson et al., 2012; Gustin et al., 2012); Davie, FL (Peterson et al., 2012; Gustin et al., 2012); and Beltsville, Maryland (MD) (Castro et al., 2012). Additional data from sites in Texas, Oklahoma, New Mexico, and Colorado were available from Sather et al.'s works (Sather et al., 2013, 2014, 2021). Data from Svalbard, Norway were also used in this comparison (Osterwalder et al., 2021). Site coordinates, elevations, dates of measurements, and reported dry deposition can be found in Table S1.

#### 2.2. Field sites - new data

Data were collected at Guadalupe Mountains National Park, TX from 7/6/2021 to 3/29/2022. This park is downwind of the Permian Basin, where oil and natural gas recovery occurs, with fracking being a common process. The park consists of a Permian carbonate reef. There is a fish consumption advisory for the trout that live in a small stream in the park, though the reef has no Hg contamination. Triplicate Aerohead samplers were deployed at the park, along with a RMAS that measured reactive Hg (RM = PBM + Hg^II).

Amsterdam Island (AMS), a station in the Global Mercury Observation System (now integrated in GOS4M, Global Observation System for Mercury, a GEO flagship aimed to support the Minamata Convention on Mercury) is a volcanic island located in the Southern Indian Ocean, 3200 km from Australia, 2880 km from Reunion Island, 4200 km from South Africa, and 3300 km from the Antarctic coast. Three Aerohead samplers were deployed, along with a RMAS that measured RM, from 12/2020 to 1/2022. Atmospheric measurements were performed at the Pointe Bénédicte research station. Additional information regarding data collected from these locations is available in Gustin et al. (2023).

## 2.3. Aerohead sampler

Dry deposition for all studies was measured using triplicate Aerohead samplers designed at the University of Nevada, Reno (Lyman et al., 2009). The Aerohead sampler is an aerodynamic polyoxymethylene disk with an etched curve to prevent precipitation and condensation from interacting with the membrane sampling surface (See graphical abstract). Sheets of CEM used to capture Hg $^{\rm II}$  (0.8  $\mu m$  pore size; Mustang-S, Pall Corporation®) were cut to fit on the sampling surface (104 cm $^2$ ), that is positioned to face down. Deposition is calculated as follows:

$$D = [(S - B) \div A] \div T, \tag{3}$$

where D is deposition (ng m $^{-2}$  h $^{-1}$ ), S is the mass of Hg on the membrane (ng Hg), B is the mass of Hg on the blank membrane(s) that travels with the samples and is placed in its own sample jar (ng Hg), A is the surface area of the membrane sampling area (m $^2$ ), and T is the duration of the deployment (h). Typical deployment times are for two weeks; however, in some cases one-week deployments occurred. The CEM does not collect GEM (Miller et al., 2019), and as deployed in the Aerohead collects little PBM as discussed below. For additional details, see the Supplemental Information.

# 2.4. Reactive Mercury Active System

The RMAS is designed to hold six dual- or triple-stage perfluoroalkoxy alkane filter packs in an anodized aluminum weather shield. Flow rates, controlled by critical flow orifices at 1 or 2 L min<sup>-1</sup>, were checked at the beginning and end of each deployment. The critical flow orifices separate the filter packs from vacuum pumps. Volumetric

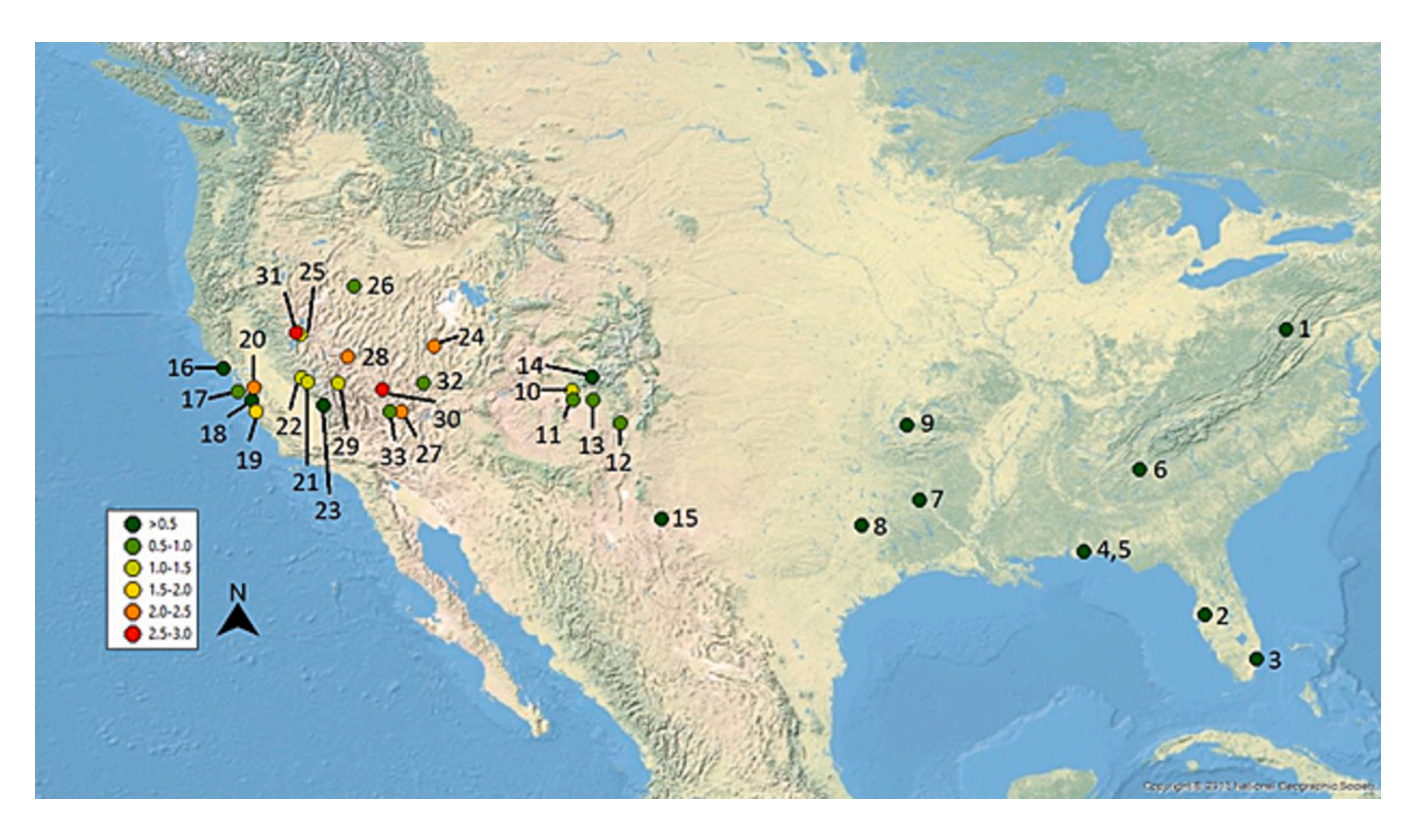


Fig. 1. Map showing locations where the Aerohead samplers have been deployed in the conterminous USA. Mean deposition rates are color-coded. Data are presented in Table S1. Sampling locations are given as numbers beside the symbols. 1) Piney Creek Reservoir, MD; 2) Tampa, FL; 3) Davie, FL; 4, 5) Outlying Landing Field, near Pensacola, FL; 6) Yorkville, GA; 7) Karnack, TX; 8) Fort Parker State Park, TX; 9) Stillwater, OK; 10) Mesa Verde National Park, CO; 11) Farmington, NM; 12) Valles Caldera National Preserve, NM; 13) Navajo Lake, NM; 14) Molas Pass, CO; 15) Guadalupe Mountains National Park, TX; 16) Point Reyes National Seashore, CA; 17) Chalk Mountain, CA; 18) Elkhorn Slough, CA; 19) Chews Ridge, CA; 20) Lick Observatory, CA; 21) Yosemite National Park, CA; 22) Hetch Hetchy Reservoir, CA; 23) Sequoia National Park, CA; 24) Great Basin National Park, NV; 25) Reno, NV; 26) Paradise Valley, NV; 27) Angel Peak, NV; 28) Berlin Ichthyosaur State Park, NV; 29) Mount Charleston, NV; 30) Echo Summit, NV; 31) Peavine Peak, NV; 32) Cathedral Gorge State Park, NV; and 33) Pahrump, NV.

flow measurements were normalized to represent air flow at standard temperature and pressure conditions (0 °C, 1 atm). CEM were used to collect RM and determine concentrations, and nylon membranes (polyamide; 0.2  $\mu m$  pore size, Sartorius Stedium Biotech) were used to estimate RM chemistry. Two CEM or nylon membranes were in each filter pack, allowing for the calculation of breakthrough. Membranes were collected and deployed using clean handling methods. For more details, see Luippold et al. (2020), Allen et al. (2023), and the Supplemental Information.

# 2.5. Analytical methods

Total Hg on CEM, downstream nylon membranes, and all blank membranes was quantified after digestion (modified EPA Method 1631) by a cold vapor atomic fluorescence spectrometer (Tekran 2600-IVS; for details, see Luippold et al., 2020). For details, see the Supplemental Information.

Upstream nylon membranes were used for thermal desorption analysis to determine the chemistry of the  ${\rm Hg^{II}}$  compounds. Desorption of  ${\rm Hg^{II}}$  compounds from nylon membranes was achieved by pulling Hgfree air through a tube furnace that houses the nylon membrane sample, then through a thermolyzer and into a Tekran 2537 (for details, see Luippold et al., 2020 and Allen et al., 2023 Supplemental Information). The tube furnace was ramp heated, and  ${\rm Hg^{II}}$  compounds are identified by the temperature range of desorption relative to standard compounds. The ranges used in this study were: 82.5–92.5 °C for [0], 95–115 °C for [Br/CI], 117.5–127.5 °C for [N], 130–147.5 °C for [S], and 150–190 °C for organic-bound compounds (Dunham-Cheatham et al., 2023).

## 3. Results and discussion

# 3.1. Field sites with published data

Lyman et al. (2007) reported dry deposition rates determined using rectangular plates with CEM surfaces facing downward. The authors found that measured deposition rates were three times higher than that determined using Tekran-derived Hg<sup>II</sup> concentrations and a dry deposition model. However, in their study, the wrong side of the membrane was exposed and values were lower than they would have been with the right side out (Lyman et al., 2009). In addition, the rectangular mounts generated more turbulence resulting in more Hg<sup>II</sup> being deposited relative to the Aerohead sampler (Lyman et al., 2009).

Lyman et al. (2009) described further development of surrogate surfaces for measurement of dry deposition. Through permeation of  $HgCl_2$ ,  $HgBr_2$ , and HgO vapors into a chamber with membranes, they determined that CEM collected these compounds with equal efficiency. This was also observed in Huang et al. (2013). In addition, by comparing ambient meteorological conditions with dry deposition rates, they determined that deposition to the membrane was not influenced by temperature, humidity, nor ozone concentrations. Dry deposition of  $Hg^{II}$  was correlated with  $Hg^{II}$  concentrations measured by Tekran 1130 units in the field. This relationship was described as:

$$\begin{split} \text{Dry deposition} \left( \text{ng m}^{-2} \, \text{h}^{-1} \right) &= 0.007 \left( \text{Tekran Hg}^{\text{II}} \, \text{concentrations} \left( \text{pg m}^{-3} \right) \right) \left( \text{r}^2 \right. \\ &= 0.9, \text{p} < 0.001, \text{n} = 326 \right). \end{split} \tag{4}$$

Data reported in Lyman et al. (2009) for two sites in Nevada and two in Florida were blank-corrected by 0.2 ng m $^{-2}$  h $^{-1}$  based on the assumption that when the Tekran Hg $^{\rm II}$  values were < 1 pg m $^{-3}$ , Hg on the membrane was from contamination from the mount. Since we now know that Tekran RM measurements are biased low, this correction factor is not valid. Thus, the blank correction of 0.2 was removed in development of Eq. (4) and for the data in Table S1.

Castro et al. (2012) reported on dry deposition using the Aerohead sampler for a forested location in Maryland impacted by Hg-emitting

industries. They overlaid their data on results from Lyman et al. (2009), and found the trend was consistent, and suggested that the Aerohead sampler may be a useful and robust method to directly measure dry deposition of  ${\rm Hg}^{\rm II}$ . The authors also noted that higher atmospheric  ${\rm Hg}^{\rm II}$  concentrations measured with the Tekran system were positively correlated with dry deposition.

Peterson et al. (2012) and Gustin et al. (2012) discussed Aerohead data collected in Pensacola, Davie, and Tampa, Florida from 2009 to 2010 as part of a study to establish a Hg Total Maximum Daily Load for the state. The authors stated biweekly dry deposition was weakly correlated with the Tekran Hg<sup>II</sup> measurements, and there was little agreement for high deposition events. Recalculating the equations with the intercept through zero and removal of the 0.2 correction factor resulted in the following equations for Pensacola (Eq. (5)), Tampa (Eq. (6)), and Davie (Eq. (7)), respectively:

$$\begin{split} \text{Dry deposition} \left( \text{ng m}^{-2} \, \text{h}^{-1} \right) &= 0.07 \left( \text{Tekran Hg}^{\text{II}} \, \text{concentrations} \left( \text{pg m}^{-3} \right) \right) \left( \text{r}^2 \right. \\ &= 0.69, \text{p} < 0.001 \right) \end{split} \tag{5}$$

$$\begin{split} \text{Dry deposition} \left( \text{ng m}^{-2} \, \text{h}^{-1} \right) &= 0.10 \left( \text{Tekran Hg}^{\text{II}} \, \text{concentrations} \left( \text{pg m}^{-3} \right) \right) \left( \text{r}^2 \right. \\ &= 0.81, \text{p} < 0.001 \right) \end{split}$$

$$\begin{split} \text{Dry deposition} \left( \text{ng m}^{-2} \ \text{h}^{-1} \right) &= 0.05 \left( \text{Tekran Hg}^{\text{II}} \ \text{concentrations} \left( \text{pg m}^{-3} \right) \right) \left( \text{r}^2 \right. \\ &= 0.77, \text{p} < 0.001 \right). \end{split}$$

(7)

These relationships are different than in Eq. (4). Actual deposition cannot be determined using Tekran HgII concentrations, because we now know they are biased low and the denuder is passivated over time (Gustin et al., 2013). Based on deposition rates, wind directions, and criteria air pollutants, three sources of HgII were identified for the Florida locations, including mobile sources, local electricity-generating facilities, and transport of air from the northeastern USA. The results pointed to different chemical forms of Hg<sup>II</sup> associated with each of these sources. Using nylon membranes and an early version of the RMAS, Huang et al. (2017) demonstrated that Br/Cl, O, N, S and an unknown Hg<sup>II</sup> compound were present at the Pensacola location. Data described in Peterson et al. (2012) resulted in two major conclusions. First, Tekran Hg<sup>II</sup> concentration measurements were biased low, and second, observations pointed to the presence of multiple Hg<sup>II</sup> compounds. The latter was suggested due to the calculation of different deposition velocities to the Aerohead membranes.

Detailed analyses of data from the Florida field sites demonstrated that different chemical forms were deposited at these three locations that correlated with the sources and deposition rates, and varied by season as explained by air patterns, sources, and meteorology. For example, deposition rates were highest in the spring and lower in the summer. Higher spring values were associated with a change in synoptic wind patterns, as supported by the criteria air pollutant data, and this was the time with the highest mean wind speeds. Lowest values in the summer reflected the fact that this time period has the highest precipitation that would scrub air of some forms of  $\mathrm{Hg}^{\mathrm{II}}$  and reduce the potential for production. At the Davie location, the summer deposition rate was 0.1 ng m $^{-2}$  h $^{-1}$  and this doubled in the fall, a time period with higher SO2, NO, and NOy (the sum of NOx = NO + NO2 and all compounds that are the result of oxidation of NOx) concentrations, and lower relative humidity.

Annual deposition for the Tampa, Davie, and Pensacola sites were  $0.2 \pm 0.12$ ,  $0.18 \pm 0.12$ ,  $0.05 \pm 0.06$  ng m $^{-2}$  h $^{-1}$ , respectively (Peterson et al., 2012). At Tampa, the local influence of mobile sources on Hg $^{\rm II}$  concentrations and deposition was greatest. This site had the highest slope value for the correlation between Tekran Hg $^{\rm II}$  concentrations and surrogate surface dry deposition, suggesting higher deposition

associated with the HgII forms that were present (e.g., likely N- and Sbased, due to inputs from cars and cruise ships). At Davie, inputs from mobile sources and electrical generating facilities were important and the correlation slope was lower than that for the Tampa data. At Pensacola, the least impacted site, mobile source impacts were lowest, and there did not appear to be a significant dry deposition component from the nearby coal-fired power plant. The correlation slope for this location was slightly higher than that for Davie. The highest dry deposition occurred in the spring at Pensacola and Tampa. At Davie, the highest values of dry deposition occurred in the spring and fall, reflecting an additional input of  $Hg^{II}$  to the area associated with regional and longrange transport, and free troposphere inputs associated with passing frontal systems. Results from these sites demonstrated that the Aerohead sampler could be used to measure deposition in areas with low HgII concentrations, and data generated are useful for determining seasonal and spatial patterns across large areas and may be used to document subtle variability, as well as identification of specific sources contributing to deposition.

Wright et al. (2014) investigated dry deposition from the Pacific Coast to eastern Nevada from July to November 2010, March to November 2011, and March to September 2012. Deposition was measured at: two locations on the California coast, Point Reves National Seashore and Elkhorn Slough; three locations in the California Coast Ranges, Chalk Mountain, Chews Ridge, and Lick Observatory; three locations in the Sierra Nevada, Yosemite National Park, Hetch Hetchy Reservoir, and Sequoia National Park; and at Great Basin National Park, on the eastern side of Nevada. Low rates of Hg dry deposition (0.3 ng  $m^{-2} h^{-1}$ ) were measured at the coastal sites, and higher rates at the high elevation locations in the Coast Ranges (1.7 to 2.4 ng m<sup>-2</sup> h<sup>-1</sup>) (Fig. 1, Table S1). Yosemite locations, including the National Park and Hetch Hetchy Reservoir, had higher deposition rates (1.2 and 1.4 ng m $^{-2}$  h $^{-1}$ ) relative to Sequoia (0.4 ng  $m^{-2} h^{-1}$ ), due to deposition to the forest at Sequoia before air masses reached the sampling site. High deposition rates were also measured at Great Basin National Park (2.2 ng m<sup>-2</sup> h<sup>-1</sup>) due to input of pollution from California and Eurasia. The low elevation coastal locations receive air primarily from the marine boundary layer, thus, 0.2 to 0.4 ng m<sup>-2</sup> h<sup>-1</sup> was estimated to be input from the marine boundary layer. Chalk Mountain was impacted by both the marine boundary layer and the free troposphere, and Wright et al. (2014) suggested that  ${\sim}0.2~\text{ng m}^{-2}~\text{h}^{-1}$  was input from long-range transport. For the high elevation coastal sites, 1 to 2 ng m<sup>-2</sup> h<sup>-1</sup> of the total measured 1.7 to 2.4 ng m $^{-2}$  h $^{-1}$  deposition rate was thought to be input via longrange transport. An elevational transect at Great Basin National Park indicated that HgII was input from the free troposphere due to longrange transport. Additional inputs to this location were from large, upwind regional population centers, such as Los Angeles.

Using surrogate surface data and available wet deposition measured by stations in the National Atmospheric Deposition Program Mercury Deposition Network, it was determined that dry deposition of  $\mathrm{Hg^{II}}$  contributed 30 % of total deposition at the coast (Wright et al., 2014). At Sequoia, dry deposition was approximately 42 % of the total Hg deposition to this site (Wright et al., 2014). At Great Basin National Park, it was estimated that ~80 % of the Hg deposited was by way of dry processes (Wright et al., 2014). This work again demonstrates how surrogate surface data allows for determining regional trends in deposition. Deposition values, along with trajectory analyses, allowed for determining contribution of different sources.

Sather et al. (2013, 2014, 2021) measured Hg dry deposition associated with the Four Corners area (intersection of Colorado, Utah, Arizona, and New Mexico) from 2009 to 2011, and then again after a coal-fired power plant in the area was decommissioned (Sather et al., 2021). Dry deposition data over time showed that regional variation in deposition influenced the whole area (Sather et al., 2014). The authors could not point to an effect of the power plant, and found an increase in Hg deposition rates at 5 locations after the power plant went off-line. They suggested the increase was due to impact of fires, cities, and oil and gas

production (Sather et al., 2021). Sather et al. (2014) noted that deposition was higher in the spring and summer relative to fall and winter. This likely reflects higher air Hg concentrations; for example, Gustin et al. (2023) reported higher Hg concentrations in Reno, NV, in the spring and summer due to long-range transport and higher convective mixing bringing Hg from the free troposphere to the surface.

Huang and Gustin (2015) reported on dry deposition measured using Aerohead samplers across 10 sites in California and Nevada. They found that deposition rates were consistently greater at elevations >2 km (Table S1). They attributed this to higher Hg<sup>II</sup> concentrations, based on measurements made with a passive Hg<sup>II</sup> sampler. Data collected with the passive sampler was applied to a relationship previously developed using Tekran-derived Hg<sup>II</sup> concentrations, using the assumption that the Tekran data were too low by 3 times the reported values. They modeled dry deposition rates using deposition velocities for HNO3 and HONO. Measured Hg<sup>II</sup> dry deposition rates did not correlate consistently with either of these compounds deposition velocities, and they suggested this meant there were different HgII forms in the air (Fig. 2). Through detailed analyses, including back trajectory analyses, the authors suggested dry deposition was impacted by Hg<sup>II</sup> chemistry. Also, based on the data, they suggested the surrogate surface simulated natural surfaces. Trajectory analyses for a high Hg deposition event for two high elevation locations demonstrated that long-range transport from Asia was the source.

In the Huang and Gustin (2015) study, they compared the commonly used membrane at the time, a medium-hydrophilic cationic polysulfone membrane (ICE 450, Pall, discontinued), to a newly developed membrane, a polyethersulfone membrane (Mustang S, Pall), and found when collecting ambient air and permeated  $HgCl_2$  and  $Hg(NO_3)_2$ ,  $Hg^{II}$  concentrations on the two surfaces were not statistically significantly different. In addition, Aeroheads using the Mustang membranes were deployed for 2- to 4-weeks, and over the same time intervals the time-weighted average dry deposition rates were not significantly different. This comparison had been done with ICE membrane (Lyman et al., 2009; Peterson et al., 2012), and showed loss if deployed for two weeks. Results of Huang and Gustin (2015) indicated the Mustang S membrane has better retention.

Osterwalder et al. (2021) deployed the Aeroheads with the CEM, along with a RMAS from March to July 2019, in order to capture Hg depletion events at the Zeppelin Observatory, located above Ny-Ålesund, Svalbard, Norway. Hg deposition rates ranged from 0.00 to 1.47 ng m<sup>-2</sup> h<sup>-1</sup>, and higher rates were associated with the depletion events. Calculated deposition velocities ranged from 0.12 to 0.49 cm s<sup>-1</sup>. Hg<sup>II</sup> compounds, identified using thermal desorption from nylon membranes, were predominantly Br/Cl and N. There was no deposition after the depletion events ended, indicating that little Hg<sup>II</sup> was present. Measured dry deposition rates were half of deposition predicted by the models; the authors attributed this to high concentrations of PBM that would not be captured on the Aerohead sampler. They demonstrated that use of the RMAS and Aerohead in tandem allowed for understanding whether RM was PBM or GOM. Since the Aerohead does not collect PBM, when the RMAS was recording data and the Aerohead membranes exhibited no concentrations, this suggested most of the RM measured by the RMAS was PBM. Calculation of RM deposition velocities for specific compounds was determined using nylon membrane data and a resistance model. Values calculated for the different compounds were the same in the model. However, based on observations discussed below, this is likely not correct. The mean deposition velocity was 0.32  $\pm$  0.09 cm s<sup>-1</sup> when the area was covered by snow, and 0.21  $\pm$  0.08 cm s<sup>-1</sup> after snowmelt. Higher deposition was observed during GEM depletion events when GOM was higher, and during this time halogenated compounds were dominant. When deposition was lower, nitrogen, sulfur, and organic compounds were greater than halogenated compounds.

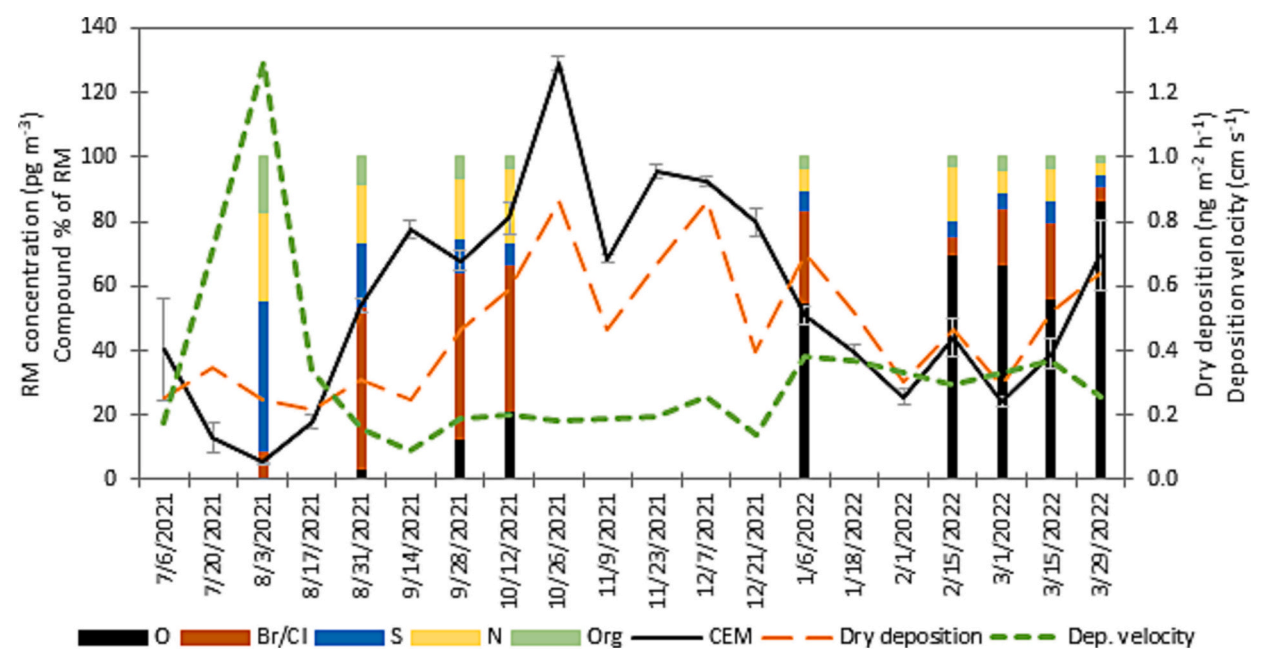


Fig. 2. Results for Guadalupe Mountains National Park, including percent of specific compounds (-O, -Br/Cl, -S, -N, -organic) in the stacked bars, and CEM Hg<sup>II</sup> concentrations (solid black curve), dry deposition (dashed orange curve), and deposition velocities (dashed green curve).

# 3.2. New field sites

Dry deposition measured at Guadalupe Mountains National Park was 0.2 to 0.8 ng m $^{-2}$  h $^{-1}$ , and lower than that measured in the Four Corners Area, with one exception (cf. Gustin et al., 2023) (Table S1; Fig. 2). Dry deposition rates were correlated with RM concentrations measured by the RMAS:

(Dry deposition (ng m
$$^{-2}$$
 h $^{-1})=0.008$  (Hg $^{II}$  concentration (pg m $^{-3})$  ) (r $^2$  
$$=0.84, p<0.001)$$
 ) (8)

with this equation being similar to the one using the data in Lyman et al. (2009). Despite the limited data, the chemistry of the compounds

influenced deposition. For example, when air was derived from the Midwest, N, S, and organic compounds were dominant and the deposition velocity was 1.3 cm s<sup>-1</sup> (n=1). When the site was impacted by long-range transport and O compounds were dominant, deposition velocities were  $0.32\pm0.05~{\rm cm~s^{-1}}$  (n=5). When halogenated compounds were present, deposition velocities were  $0.19\pm0.02~{\rm cm~s^{-1}}$  (n=3). For a presentation of RMAS and ancillary data associated with this site and for Amsterdam Island, discussed below, see Gustin et al. (2023).

At Amsterdam Island, a remote site mainly influenced by air masses from the marine boundary layer (Angot et al., 2014; Slemr et al., 2015; Slemr et al., 2020), dry deposition ranged from 0.1 to 0.4 ng m $^{-2}$  h $^{-1}$  (Fig. 3). Chemistry was predominately halogenated compounds (Fig. 3). Deposition velocities across the year of sampling ranged from 0.14 to

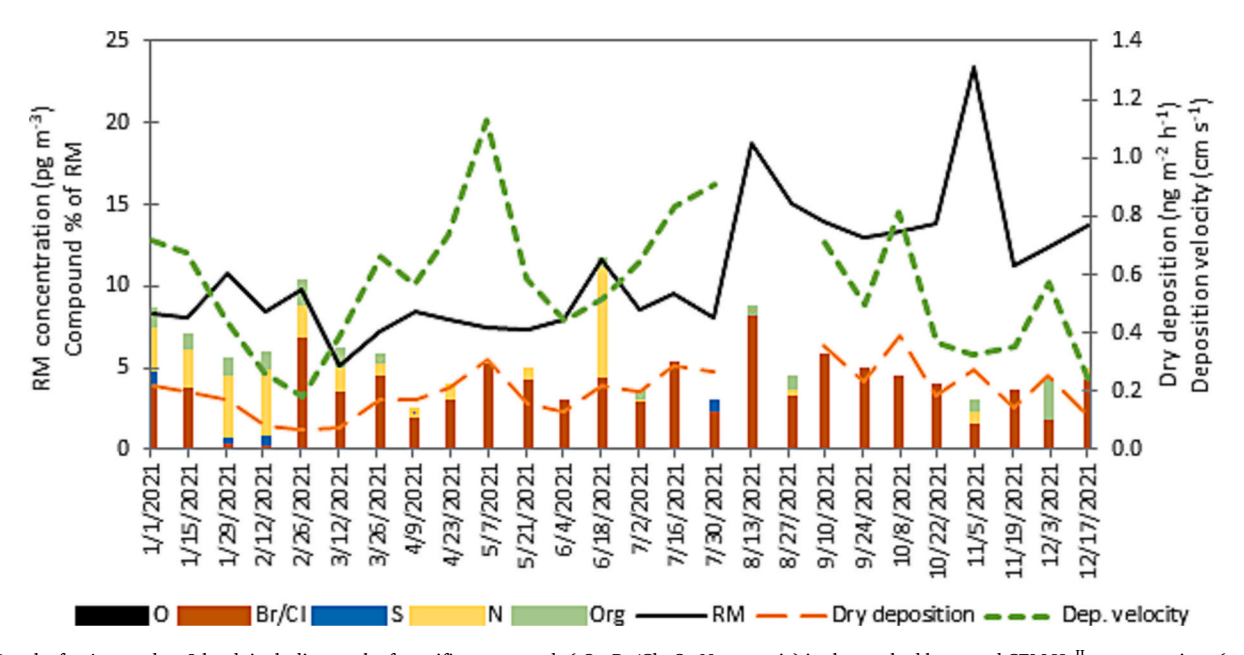


Fig. 3. Results for Amsterdam Island, including peak of specific compounds (-O, -Br/Cl, -S, -N, -organic) in the stacked bars, and CEM Hg<sup>II</sup> concentrations (solid black curve), dry deposition (dashed orange curve), and deposition velocities (dashed green curve).

 $1.3~{\rm cm~s^{-1}}$  (mean  $0.54~{\rm cm~s^{-1}}$ ; median  $0.57~{\rm cm~s^{-1}}$ ; standard deviation  $0.24~{\rm cm~s^{-1}}$ ). Deposition velocities were correlated with mean wind speed over the sampling period:

(deposition velocity (cm s<sup>-1</sup>) = 
$$12^*$$
 wind speed (m s<sup>-1</sup>) (r<sup>2</sup>  
=  $0.84$ , p <  $0.001$ ,n =  $24$ )). (9)

Dry deposition was also correlated with CEM RM concentrations:

(dry deposition = 
$$0.017^*$$
 Hg<sup>II</sup> concentration ( $r^2 = 0.78$ , p <  $0.001$ )). (10)

#### 4. Comparison of dry deposition across locations

Mean dry deposition for sampling locations is summarized in Table S1, and those for the conterminous USA depicted in Fig. 1. Dry deposition rates were measured outside the USA at two marine locations and in a major city in China with a population of  $\sim\!9.5$  million. Dry deposition rates measured at Svalbard reflected atmospheric Hg depletion events that occur with polar sunrise. The zero deposition values are due no gaseous oxidized Hg being present. On Amsterdam Island, where compounds were primarily halogenated, deposition was 0.1 to 0.4 ng m $^{-2}$  h $^{-1}$ , and Hg $^{II}$  compounds were present all year round. In Nanjing, where the chemical forms were primarily N, O, and organic (Lei Zhang, Nanjing University, personal communication), mean deposition was higher (0.64 ng m $^{-2}$  h $^{-1}$ ).

In general, deposition rates for coastal sites were similar (0.25 to 0.4 ng m $^{-2}$  h $^{-1}$ ). Using all USA locations that were located in areas unimpacted by local and regional sources, there was a weak but significant positive correlation ( $r^2=0.26$ , p=0.001) between deposition and elevation (Fig. 4). This reflects the fact that deposition will be influenced by the general location, Hg $^{II}$  compounds present, and atmospheric turbulence. However, a stronger relationship has been observed in regional studies (c.f. Huang and Gustin, 2015; Wright et al., 2014,). It is also likely that more interaction with the free troposphere in the west relative to the east results in higher RM concentrations. Looking at the data in detail, it is noteworthy that there were two data points for Paradise Valley, Nevada, one of them high and another low. The latter data were collected for 7 months (excluding summer), while the higher value reflects 2 years of sampling and is more representative of Hg $^{II}$  deposition

rates at the location. The higher deposition value for Lick Observatory was due to this location being impacted by long-range transport of Hg entering the western coast of the USA and  ${\rm Hg^{II}}$  being deposited with the first intersection with continental land masses. Low deposition rates were reported for locations in Texas (Fort Parker and Guadalupe Mountains National Park), New Mexico (Navajo Lake and Valles Caldera), and Colorado (Mesa Verde and Molas Pass). This is due to these locations being farther east and inland, and  ${\rm Hg^{II}}$  being deposited as air moves across the USA from west to east. Sather et al. (2014) presented data from Texas and Oklahoma, farther east of New Mexico for September 2011 to September 2012 deposition rates of 0.1 to 0.3 and 0.2 ng m $^{-2}$  h $^{-1}$ , respectively.

# 5. Suggestions for a path forward

The Aerohead method is a surrogate for potential dry deposition to the Earth's surfaces, including substrates, vegetation, snow, and water. However, once dry deposited to vegetation,  $Hg^{II}$  can be photoreduced and emitted back to the atmosphere as GEM or it can be washed off from surfaces. Lyman et al. (2007) demonstrated that  $Hg^{II}$  deposited to surrogate surfaces was 20 times higher than that collected by aspen foliage and 100 % higher than sagebrush.  $Hg^{II}$  deposited to snow has been shown to be readily re-emitted (Fain et al., 2013). Dry deposition to water will be driven by Henry's Law and the resistance of the stagnant film layer. Dry deposition of  $Hg^{II}$  to water can also be emitted back to the air as GEM.  $Hg^{II}$ , the form more readily methylated and dry deposited, has resulted in fish contamination in pristine ecosystems, e.g. Chen and Driscoll (2018)

Use of this method coupled with the RMAS or a dual-channel system allows for calculation of deposition velocities that are useful for modelers. Since the RMAS CEM method recorded lower concentrations than two dual-channel systems by 30 and 50 %, deposition velocities calculated using RMAS data may be biased high. Using one material, in this case the CEM, provides a framework within which comparison of deposition may be made across locations.

As demonstrated, the Aerohead is a useful method for understanding regional patterns in dry deposition, and quantifying deposition associated with specific sources. Higher deposition was observed at higher elevation relative to those at low elevation in western regional networks,

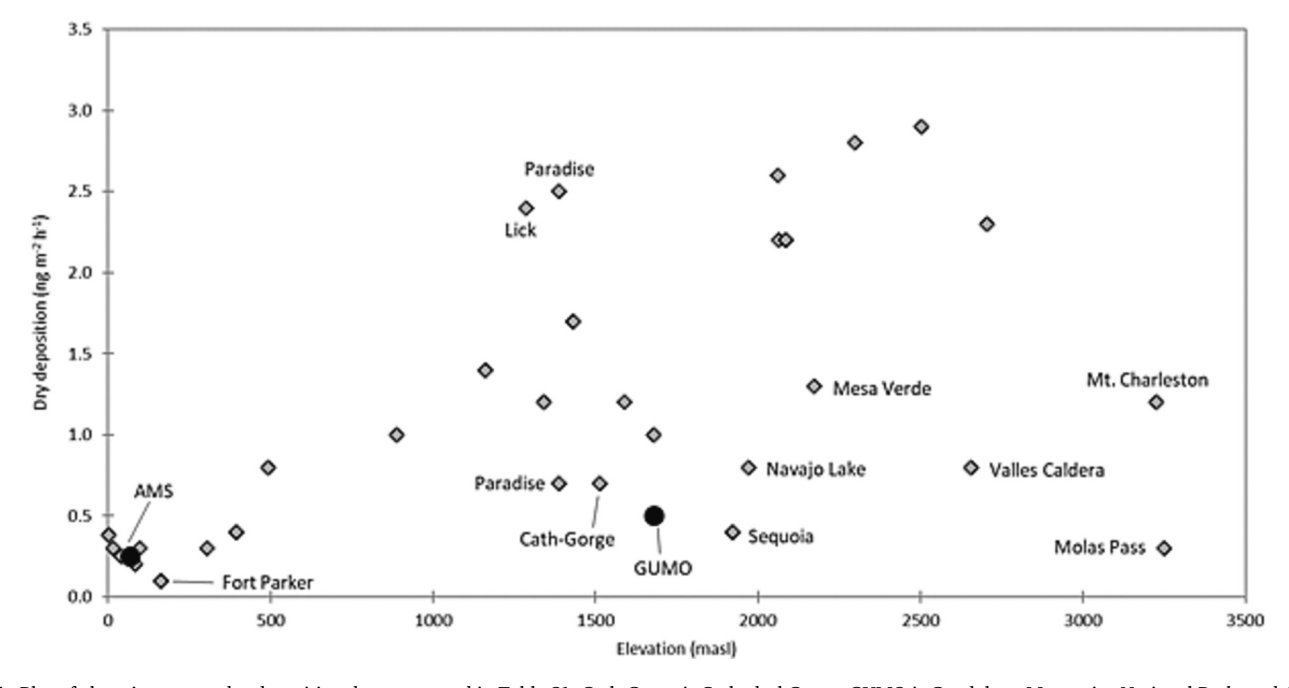


Fig. 4. Plot of elevation versus dry deposition data presented in Table S1. Cath-Gorge is Cathedral Gorge, GUMO is Guadalupe Mountains National Park, and AMS is Amsterdam Island. New sites are plotted as black dots.

and this is due to higher  $Hg^{II}$  concentrations at high elevation associated with air in the free troposphere. Trends observed with data from across the USA point to less deposition at these sampling locations that were not highly impacted by anthropogenic sources moving from west to east due to deposition of  $Hg^{II}$  to surfaces, and less interaction with the free troposphere as air masses move across the USA.

Data collected using the Aerohead and a RMAS and/or a dual-channel system can allow for calculation of deposition velocities that will be lower than those derived from using Tekran-derived Hg<sup>II</sup> concentrations. Although data are limited, with an understanding of the chemistry of the Hg<sup>II</sup> compounds and more accurate concentrations, compound-specific deposition velocities can be determined as shown by the data collected at Guadalupe Mountains National Park. More work should be done to better understand compound-specific deposition velocities. The Amsterdam Island data set, with constant chemistry and environmental conditions, clearly demonstrated deposition was influenced by wind velocity.

Direct measurement of wet and dry deposition is currently the best way to understand deposition to ecosystems, and the need to quantify inputs to ecosystems as required by the Minamata Convention. Currently, the best method to determine dry deposition is the Aerohead sampler with a CEM collection surface (Huang et al., 2014). Little work has been done to investigate alternate methods since mid 2010.

# CRediT authorship contribution statement

Mae Gustin compiled data for the review and wrote the manuscript. Sarrah Dunham-Cheatham coordinated collection of data at Guadalupe Mountains National Park and Amsterdam Island. She analyzed the samples and compiled the data and edited the manuscript.

Olivier Magand, Stefan Osterwalder, and Aurélien Dommergue coordinated the Amsterdam Island sample collection, provided ancillary data, and edited the manuscript.

# **Declaration of competing interest**

The authors declare there is no conflict of interest.

# Data availability

Data will be made available on request.

## Acknowledgements

Jiaoyan Huang read and commented on a version of this manuscript. We thank the reviewers for taking the time to comment on our manuscript. Thanks to Seth Lyman for providing data and figures from earlier papers. Thanks to undergraduate students working in the Gustin laboratory for maintaining strict QA/QC cleaning protocols. Nicole Choma helped with Table S1 and generated Fig. 1. Many thanks to overwintering people and the French Polar Institute Paul-Emile Victor (IPEV) staff and scientists who helped with the setup and maintenance of the experiment in the framework of the GMOStral-1028 IPEV program and the ICOS-AMS-416 program, at the Amsterdam Island site (TAAF territories).

Funding for the project came from the National Science Foundation Division of Atmospheric & Geospace Sciences, grant number 2043042. The U.S. Environmental Protection Agency provided limited funding for the Guadalupe Mountains National Park site, and we thank the staff there for collecting and deploying the membranes. Amsterdam Island dry deposition atmospheric mercury data, was collected with funding from the French Polar Institute IPEV via GMOStral-1028 IPEV program. SO received funding from the Swiss National Science Foundation (SNSF grant no. P400P2 180796).

#### Appendix A. Supplementary data

Supplementary data to this article can be found online at  $\frac{\text{https:}}{\text{doi.}}$  org/10.1016/j.scitotenv.2023.167895.

#### References

- Allen, N., Gacnik, J., Dunham-Cheatham, S.M., Gustin, M.S., 2023. Tests of alternate membranes an alternate configuration for the Reactive Mercury Active System. Atmos. Environ. (Revised and resubmitted).
- Angot, H., Barret, M., Magand, O., Ramonet, M., Dommergue, A., 2014. A 2-year record of atmospheric mercury species at a background Southern Hemisphere station on Amsterdam Island. Atmos. Chem. Phys. 14 (20), 11461–11473. https://doi.org/ 10.5194/acp-14-11461-2014.
- Caldwell, C.A., Swartzendruber, P., Prestbo, E., 2006. Concentration and dry deposition of mercury species in arid south Central New Mexico (2001–2002). Environ. Sci. Technol. 40 (24), 7535–7540. https://doi.org/10.1021/es0609957.
- Castro, M.S., Moore, C., Sherwell, J., Brooks, S.B., 2012. Dry deposition of gaseous oxidized mercury in western Maryland. Sci. Total Environ. 417, 232–240. https:// doi.org/10.1016/j.scitotenv.2011.12.044.
- Chen, C.Y., Driscoll, C.T., 2018. Integrating mercury research and policy in a changing world. Ambio 47, 111–115.
- Dunham-Cheatham, S.M., Lyman, S., Gustin, M.S., 2023. Comparison and calibration of methods for ambient reactive mercury quantification. Sci. Total Environ. 856. https://doi.org/10.1016/j.scitotenv.2022.159219.
- Fain, X., Helmig, D., Hueber, J., Obrist, D., Williams, M.W., 2013. Mercury dynamics in the Rocky Mountain, Colorado, snowpack. Biogeosciences 10, 3793–3807.
- Fang, G.C., Lin, Y.H., Chang, C.Y., 2013. Use of mercury dry deposition samplers to quantify dry deposition of particulate-bound mercury and reactive gaseous mercury at a traffic sampling site. Environ. Forensic 14 (3), 182–186. https://doi.org/ 10.1080/15275922.2013.814177.
- Gustin, M.S., Weiss-Penzias, P.S., Peterson, C., 2012. Investigating sources of gaseous oxidized mercury in dry deposition at three sites across Florida, USA. Atmos. Chem. Phys. 12 (19), 9201–9219. https://doi.org/10.5194/acp-12-9201-2012.
- Gustin, M.S., Huang, J.Y., Miller, M.B., Peterson, C., Jaffe, D.A., Ambrose, J., Finley, B. D., Lyman, S.N., Call, K., Talbot, R., Feddersen, D., Mao, H., Lindberg, S.E., 2013. Do we understand what the mercury speciation instruments are actually measuring? Results of RAMIX. Environ. Sci. Technol. 47 (13), 7295–7306. https://doi.org/10.1021/es3039104.
- Gustin, M.S., Allen, N., Cheatham, Dunham, Choma, N., Lyman, S.N., Johnson, W., Lopez, S., Russell, A., Mei, E., Magand, O., Dommergue, A., 2023. Observations of the chemistry and concentrations of reactive Hg at locations with different ambient air chemistry. Sci. Total Environ. 904. 16618.
- Gustin, M.S., Dunham-Cheatham, S.M., Choma, N., Shoemaker, K., Allen, N., 2023. Determining sources of reactive mercury compounds in Reno, Nevada, United States. Front. Environ. Chem. 4, 1202957. https://doi.org/10.3389/fenvc.2023.1202957.
- Hall, N.L., Dvonch, J.T., Marsik, F.J., Barres, J.A., Landis, M.S., 2017. An artificial turf-based surrogate surface collector for the direct measurement of atmospheric mercury dry deposition. Int. J. Environ. Res. Public Health 14 (2). https://doi.org/10.3390/ijerph14020173.
- Huang, J.Y., Gustin, M.S., 2015. Use of passive sampling methods and models to understand sources of mercury deposition to high elevation sites in the western United States. Environ. Sci. Technol. 49 (1), 432–441. https://doi.org/10.1021/es502836w.
- Huang, J.Y., Liu, Y., Holsen, T.M., 2011. Comparison between knife-edge and frisbee-shaped surrogate surfaces for making dry deposition measurements: wind tunnel experiments and computational fluid dynamics (CFD) modeling. Atmos. Environ. 45 (25), 4213–4219. https://doi.org/10.1016/j.atmosenv.2011.05.013.
- Huang, J.Y., Miller, M.B., Weiss-Penzias, P., Gustin, M.S., 2013. Comparison of gaseous oxidized hg measured by KCl-coated denuders, and nylon and cation exchange membranes. Environ. Sci. Technol. 47 (13), 7307–7316. https://doi.org/10.1021/ oc/01/340
- Huang, J.Y., Lyman, S.N., Hartman, J.S., Gustin, M.S., 2014. A review of passive sampling systems for ambient air mercury measurements. Environ. Sci.: Process. Impacts 16 (3), 374–392. https://doi.org/10.1039/c3em00501a.
- Huang, J.Y., Miller, M.B., Edgerton, E., Gustin, M.S., 2017. Deciphering potential chemical compounds of gaseous oxidized mercury in Florida, USA. Atmos. Chem. Phys. 17 (3), 1689–1698. https://doi.org/10.5194/acp-17-1689-2017.
- Luippold, A., Gustin, M.S., Dunham-Cheatham, S.M., Zhang, L., 2020. Improvement of quantification and identification of atmospheric reactive mercury. Atmos. Environ. 224. https://doi.org/10.1016/j.atmosenv.2020.117307.
- Lyman, S.N., Gustin, M.S., Prestbo, E.M., Marsik, F.J., 2007. Estimation of dry deposition of atmospheric mercury in Nevada by direct and indirect methods. Environ. Sci. Technol. 41 (6), 1970–1976. https://doi.org/10.1021/es062323m.
- Lyman, S.N., Gustin, M.S., Prestbo, E.M., Kilner, P.I., Edgerton, E., Hartsell, B., 2009. Testing and application of surrogate surfaces for understanding potential gaseous oxidized mercury dry deposition. Environ. Sci. Technol. 43, 6235–6241.
- Miller, M.B., Dunham-Cheatham, S.M., Gustin, M.S., Edwards, G.C., 2019. Evaluation of cation exchange membrane performance under exposure to high Hg-0 and HgBr2 concentrations. Atmos. Meas. Tech. 12, 1207–1217.
- Osterwalder, S., Dunham-Cheatham, S.M., Araujo, B.F., Magand, O., Thomas, J.L., Baladima, F., Pfaffhuber, K.A., Berg, T., Zhang, L., Huang, J.Y., Dommergue, A., Sonke, J.E., Gustin, M.S., 2021. Fate of springtime atmospheric reactive mercury:

- concentrations and deposition at Zeppelin, Svalbard. ACS Earth Space Chem. 5 (11), 3234–3246. https://doi.org/10.1021/acsearthspacechem.1c00299.
- Peterson, C., Alishahi, M., Gustin, M.S., 2012. Testing the use of passive sampling systems for understanding air mercury concentrations and dry deposition across Florida, USA. Sci. Total Environ. 424, 297–307. https://doi.org/10.1016/j.scitotenv.2012.02.031.
- Prestbo, E.M., Gay, D.A., 2009. Wet deposition of mercury in the U.S. and Canada, 1996-2005: results and analysis of the NADP mercury deposition network (MDN). Atmos. Environ. 43 (27), 4223–4233. https://doi.org/10.1016/j.atmosenv.2009.05.028.
- Sakata, M., Marumoto, K., 2005. Wet and dry deposition fluxes of mercury in Japan. Atmos. Environ. 39 (17), 3139–3146. https://doi.org/10.1016/j.atmosenv.2005.01.049
- Sather, M.E., Mukerjee, S., Smith, L., Mathew, J., Jackson, C., Callison, R., Scrapper, L., Hathcoat, A., Adam, J., Keese, D., Ketcher, P., Brunette, R., Karlstrom, J., Van der Jagt, G., 2013. Gaseous oxidized mercury dry deposition measurements in the Four Corners area and Eastern Oklahoma, U.S.A. Atmos. Pollut. Res. 4 (2), 168–180. https://doi.org/10.5094/apr.2013.017.
- Sather, M.E., Mukerjee, S., Allen, K.L., Smith, L., Mathew, J., Jackson, C., Callison, R., Scrapper, L., Hathcoat, A., Adam, J., Keese, D., Ketcher, P., Brunette, R., Karlstrom, J., Van der Jagt, G., 2014. Gaseous oxidized mercury dry deposition measurements in the southwestern USA: a comparison between Texas, eastern Oklahoma, and the four corners area. Sci. World J. 5580723. https://doi.org/10.1155/2014/580723.
- Sather, M.E., Mukerjee, S., Smith, L., Mathew, J., Jackson, C., Flournoy, M., 2021. Gaseous oxidized mercury dry deposition measurements in the Four Corners area, U. S.A., after large power plant mercury emission reductions. Atmos. Pollut. Res. 12 (1), 148–158. https://doi.org/10.1016/j.apr.2020.08.030.
- Slemr, F., Angot, H., Dommergue, A., Magand, O., Barret, M., Weigelt, A., Ebinghaus, R., Brunke, E.G., Pfaffhuber, K.A., Edwards, G., Howard, D., Powell, J., Keywood, M., Wang, F., 2015. Comparison of mercury concentrations measured at several sites in the Southern Hensiphere. Atmos. Chem. Phys. 15 (6), 3125–3133. https://doi.org/10.5194/acp-15-3125-2015.

- Slemr, F., Martin, L., Labuschagne, C., Mkololo, T., Angot, H., Magand, O., Dommergue, A., Garat, P., Ramonet, M., Bieser, J., 2020. Atmospheric mercury in the southern hemisphere - part 1: trend and inter-annual variations in atmospheric mercury at Cape Point, South Africa, in 2007-2017, and on Amsterdam Island in 2012-2017. Atmos. Chem. Phys. 20 (13), 7683–7692. https://doi.org/10.5194/acp-20-7683-2020.
- Sprovieri, F., Pirrone, N., Bencardino, M., D'Amore, F., Angot, H., Barbante, C., Brunke, E.G., Arcega-Cabrera, F., Cairns, W., Comero, S., del Carmen Diéguez, M., Dommergue, A., Ebinghaus, R., Feng, X.B., Fu, X., et al., 2017. Five-year records of mercury wet deposition flux at GMOs sites in the Northern and Southern hemispheres. Atmos. Chem. Phys. 17 (4), 2689–2708. https://doi.org/10.5194/acp-17-2689-2017.
- Talbot, R., Mao, H.T., Feddersen, D., Smith, M., Kim, S.Y., Sive, B., Haase, K., Ambrose, J., Zhou, Y., Russo, R., 2011. Comparison of particulate mercury measured with manual and automated methods. Atmosphere 2 (1), 1–20. https://doi.org/ 10.3390/atmos/2010001
- Wright, G., Gustin, M.S., Weiss-Penzias, P., Miller, M.B., 2014. Investigation of mercury deposition and potential sources at six sites from the Pacific Coast to the Great Basin, USA. Sci. Total Environ. 470, 1099–1113. https://doi.org/10.1016/j. scitotenv.2013.10.071.
- Zhang, L., Wright, L.P., Blanchard, P., 2009. A review of current knowledge concerning dry deposition of atmospheric mercury. Atmos. Environ. 43 (37), 5853–5864. https://doi.org/10.1016/j.atmosenv.2009.08.019.
- Zhang, L., Zhou, P.S., Cao, S.Z., Zhao, Y., 2019. Atmospheric mercury deposition over the land surfaces and the associated uncertainties in observations and simulations: a critical review. Atmos. Chem. Phys. 19 (24), 15587–15608. https://doi.org/ 10.5194/acp-19-15587-2019.
- Zhang, L., Zhang, G.C., Zhou, P.S., Zhao, Y., 2023. A review of dry deposition schemes for speciated atmospheric mercury. Bull. Environ. Contam. Toxicol. 110 (1) https://doi. org/10.1007/s00128-022-03641-0.